Journal of
Applied Remote Sensing

RemoteSensing.SPIEDigitalLibrary.org

Advances of the smooth variable structure filter: square-root and two-pass formulations

S. Andrew Gadsden
Andrew S. Lee

S. Andrew Gadsden, Andrew S. Lee, "Advances of the smooth variable structure filter: square-root and two-pass formulations," *J. Appl. Remote Sens.* **11**(1), 015018 (2017), doi: 10.1117/1.JRS.11.015018.

Advances of the smooth variable structure filter: square-root and two-pass formulations

S. Andrew Gadsden[a,*] **and Andrew S. Lee**[a,b]
[a]University of Guelph, School of Engineering, Guelph, Ontario, Canada
[b]University of Maryland, Department of Mechanical Engineering, Baltimore, Maryland, United States

Abstract. The smooth variable structure filter (SVSF) has seen significant development and research activity in recent years. It is based on sliding mode concepts, which utilize a switching gain that brings an inherent amount of stability to the estimation process. In an effort to improve upon the numerical stability of the SVSF, a square-root formulation is derived. The square-root SVSF is based on Potter's algorithm. The proposed formulation is computationally more efficient and reduces the risks of failure due to numerical instability. The new strategy is applied on target tracking scenarios for the purposes of state estimation, and the results are compared with the popular Kalman filter. In addition, the SVSF is reformulated to present a two-pass smoother based on the SVSF gain. The proposed method is applied on an aerospace flight surface actuator, and the results are compared with the Kalman-based two-pass smoother. © *2017 Society of Photo-Optical Instrumentation Engineers (SPIE)* [DOI: 10.1117/1.JRS.11.015018]

Keywords: Kalman filter; smooth variable structure filter; square root; minimum variance; smoother; target tracking.

Paper 16179P received Mar. 7, 2016; accepted for publication Feb. 13, 2017; published online Mar. 9, 2017.

1 Introduction

State and parameter estimation theory is an important field in mechanical and electrical engineering. As the name suggests, estimation strategies are used to predict, estimate, or smooth out important system states and parameters.[1,2] Consider a simple example, a spring-damper-mass system. To accurately control and understand the dynamics of the system, an engineer or scientist must have an accurate representation of the spring constant, damper value, and system mass. If these values are not known with a degree of certainty, then the system will be modeled incorrectly and the dynamics will lead to instability or system failure.[3,4] Estimation strategies are used to identify these state and parameter values. Filters use measurements and system information taken at time t to estimate state values at time t. However, smoothers estimate the state of a system at time t using information before and after time t. The accuracy of a smoother is generally better than that of a filter since it makes use of more information for its estimate. As per Refs. 5 and 6, there are three types of smoothers: fixed-interval, fixed-point, and fixed-lag. Fixed-interval smoothers are often used offline and use all the measurements over a fixed interval to estimate the system states throughout the entire interval. Fixed-point smoothers estimate the state at a fixed time in the past. Fixed-lag smoothers estimate states at a fixed time interval at some point behind the current measurement (hence, lag).

The most popular estimation strategy was developed nearly 60 years ago and is referred to as the Kalman filter (KF).[7] The KF yields a statistically optimal solution to the linear estimation problem. The goal of the KF is to minimize the state error covariance, which is a measure of the estimation accuracy and is defined as the expectation of the state error squared.[7] The state error is defined as the difference between the true state value and the estimation state value. Although the KF yields a solution for linear estimation problems, it is based on a few strict assumptions: the

*Address all correspondence to: S. Andrew Gadsden, E-mail: gadsden@uoguelph.ca

system and measurement models must be known, the noise distribution is Gaussian, and the behavior is linear.[4,6] If any of these assumptions are not held by the actual system, then the KF may yield inaccurate or unstable estimation results.[8,9] Other KF-based solutions have been presented to overcome issues with nonlinearity: the perturbation KF, the extended Kalman filter (EKF), the unscented Kalman filter (UKF), and the cubature Kalman filter (CKF).[8,10–12] Essentially, these solutions attempt to linearize or approximate the nonlinearities, with increasing degrees of complexity. For example, the EKF is a first-order Taylor series approximate, the UKF is equivalent to a second-order approximation, and the CKF is equivalent to a third-order approximation.[8] Although these methodologies are distinctly different and offer improved estimation accuracy, they still fall victim to modeling uncertainties and external, unwanted disturbances—which is often the case in real-world scenarios and estimation problems.

Over the years, estimation strategies such as the H-infinity filter and the smooth variable structure filter (SVSF) have been introduced to overcome modeling uncertainties and errors.[13–17] However, a trade-off often exists between accuracy and robustness. The SVSF was introduced in 2007 and was considered to be a suboptimal filter albeit stable and robust.[16] It is based on sliding mode concepts that yields a switching gain. This gain brings an inherent amount of stability to the estimation process as the estimates are forced toward the true state trajectory. Improvements were made on this format and newer forms of the SVSF were introduced, including covariance derivations, multiple-model formulations, a time-varying boundary layer solution, and combined KF-based derivations.[8,9,11,18] A number of applications were considered, including target tracking, fault detection and diagnosis, system control, and basic state and parameter estimation examples.[8,19–22] Although the SVSF has shown significant improvement since its introduction, it remains a suboptimal filter and has room for advancement.

As described in Ref. 9, square-root (or factored-form) filters help to ensure numerical stability.[23–25] The square-root formulation makes use of three powerful linear algebra techniques: QR decomposition, Cholesky factor updating, and efficient least squares.[26,27] The covariance matrix is broken up into factored terms, which are propagated forward and updated at each measurement.[5] The factors are multiplied together to reform the covariance matrix, thus ensuring it to be positive definite. The two most popular square-root filters are Potter's square-root filter and Bierman–Thornton's UD filter.[28] The UD filter has similar accuracy to Potter's strategy; however, it is less computationally expensive.[6] Introduced in the late 1970s, UD filtering is based on transformation methods that involve an upper triangle covariance factorization [Eq.(1)].[29,30] Although the UD strategy is considered a type of square-root filter, no square roots are actually calculated; the covariance P is defined by

$$P = \mathrm{UDU}^{\mathrm{T}}, \tag{1}$$

where U is an upper triangle matrix with diagonal elements that are unity (all 1) and $D = \mathrm{diag}(d_1, \ldots, d_n)$. The matrices U and D are referred to as the UD factors of the covariance matrix P. A number of different strategies exist to perform UD decomposition (i.e., to create U and D matrices).[2] Further, in the UD strategy, numerical stability for filtering strategies can be improved by factoring the covariance matrix into Cholesky factors.[31] This was discovered when attempting to improve the stability of the KF when dealing with finite-precision arithmetic.[2] Essentially the nature of the KF remains the same; however, an equivalent statistical parameter is used and is found to be less sensitive to round-off errors.[32] Increasing the arithmetic precision reduces the effects of round-off error, which improves the overall stability of the filter.

This paper is organized as follows. KF and SVSF and their equations are summarized in Sec. 2. The square-root formulations of the KF are shown in Sec. 3, and the square-root SVSF is then summarized. The two-pass formulations of the KF and SVSF are shown in Sec. 4. In Sec. 5, the target tracking scenario is described, and the results of implementing the square-root KF and square-root SVSF are shown and compared. In Sec. 6, the aerospace actuator scenario is described, and the results of implementing the two-pass KF-based smoother and two-pass SVSF-based smoother are shown and compared. The paper is then concluded, and future work is described.

2 Estimation Strategies

2.1 *Kalman Filter*

The following equations form the core of the KF algorithm and are used in an iterative fashion. Equations (2) and (3) define the *a priori* state estimate $\hat{x}_{k+1|k}$, based on knowledge of the system F and previous state estimate $\hat{x}_{k|k}$, and the corresponding state error covariance matrix $P_{k+1|k}$, respectively

$$\hat{x}_{k+1|k} = F\hat{x}_{k|k} + Gu_k, \tag{2}$$

$$P_{k+1|k} = FP_{k|k}F^{\mathrm{T}} + Q_{k.} \tag{3}$$

The Kalman gain K_{k+1} is defined by Eq. (4) and is used to update the state estimate $\hat{x}_{k+1|k+1}$ as shown in Eq. (5). The gain makes use of an innovation covariance S_{k+1}, which is defined as the inverse term found in the following equation:

$$K_{k+1} = P_{k+1|k}H^{\mathrm{T}}(HP_{k+1|k}H^{\mathrm{T}} + R_{k+1})^{-1}, \tag{4}$$

$$\hat{x}_{k+1|k+1} = \hat{x}_{k+1|k} + K_{k+1}(z_{k+1} - H\hat{x}_{k+1|k}). \tag{5}$$

The *a posteriori* state error covariance matrix $P_{k+1|k+1}$ is then calculated by Eq. (6) and is used iteratively, as per Eq. (3)

$$P_{k+1|k+1} = (I - K_{k+1}H)P_{k+1|k}(I - K_{k+1}H)^{\mathrm{T}} + K_{k+1}R_{k+1}K^{\mathrm{T}}_{k+1.} \tag{6}$$

The derivation of the KF is well documented, with details available in Refs. 1, 3, and 7. The KF gain is unique as it yields an optimal solution to the linear estimation problem; however, it comes at a price of stability and robustness. Assumptions used in the derivation include: the system model is known and linear, the system and measurement noises are white, and the states have initial conditions with known means and variances.[4,6] However, the previous assumptions often do not hold in a number of applications. If these assumptions are violated, the KF yields suboptimal results and can become unstable.[10] In addition, the KF is sensitive to computer precision and the complexity of computations involving matrix inversions.[2] However, modern computing power has reduced this drawback significantly. The EKF is a natural extension of the KF method. However, the EKF may be used for nonlinear systems and measurements, unlike the KF. A nonlinear system or measurement equation may be linearized according to its Jacobian. The partial derivatives are used to compute linearized system and measurement matrices F and H, respectively, found as follows:[33]

$$F_k = \frac{\partial f}{\partial x}\bigg|_{\hat{x}_{k|k},u_k}, \tag{7}$$

$$H_{k+1} = \frac{\partial h}{\partial x}\bigg|_{\hat{x}_{k+1|k}}. \tag{8}$$

Note that the nonlinear system equation is represented by f and the nonlinear measurement equation is represented by h. Equations (7) and (8) essentially linearize the nonlinear system or measurement functions around the current state estimate.[1] These values can then be used as per Eqs. (2)–(6). This comes at a loss of optimality; as such, the EKF yields a suboptimal solution to the nonlinear estimation problem.[3] Other Kalman-based methods exist beyond the EKF, such as the UKF and the CKF.[11] Although these methods yield improvements on the EKF, a number of strict assumptions still apply. Modeling errors, uncertainties, and disturbances can still lead to unstable estimates.

2.2 *Smooth Variable Structure Filter*

The SVSF was derived in 2007 and has been shown to be stable and robust to bounded disturbances, modeling uncertainties, and noise.[14,15] The basic estimation concept of the SVSF is shown in Fig. 1.

The SVSF method is model based and may be applied to differentiable linear or nonlinear dynamic system models.[34,35] The original form of the SVSF as presented in Ref. 16 did not include covariance derivations. An augmented form of the SVSF was presented in Refs. 8 and 9, which proposed a strategy for obtaining an error covariance matrix for the filter. The estimation process is iterative and may be summarized by the following set of equations. The predicted state estimates $\hat{x}_{k+1|k}$ and the error covariance matrix $P_{k+1|k}$ are first calculated as per the KF strategy.

Utilizing the predicted state estimates $\hat{x}_{k+1|k}$, the predicted measurements $\hat{z}_{k+1|k}$, and the measurement errors $e_{z,k+1|k}$ may be calculated by Eqs. (9) and (10), respectively

$$\hat{z}_{k+1|k} = H\hat{x}_{k+1|k}, \tag{9}$$

$$e_{z,k+1|k} = z_{k+1} - \hat{z}_{k+1|k.} \tag{10}$$

Notice how Eqs. (9) and (10) are similar to the KF.[36] The SVSF process differs in how the gain is formulated. The SVSF gain is a function of the *a priori* and the *a posteriori* measurement errors $e_{z,k+1|k}$ and $e_{z,k|k}$; the smoothing boundary layer widths ψ; the SVSF "memory" or convergence rate γ; and the measurement matrix C. Refer to Refs. 9 and 16 for a complete explanation on how the gain K_{k+1} is derived. The SVSF gain is defined as a diagonal matrix such that[8]

$$K_{k+1} = C^{+}\mathrm{diag}[(|e_{z,k+1|k}| + \gamma|e_{z,k|k}|)\mathrm{sat}(\bar{\psi}^{-1}e_{z,k+1|k})]\mathrm{diag}(e_{z,k+1|k})^{-1}. \tag{11}$$

The smoothing boundary layer term $\bar{\psi}$ in Eq. (11) is defined as

$$\bar{\psi}^{-1} = \begin{bmatrix} \frac{1}{\psi_1} & 0 & 0 \\ 0 & \ddots & 0 \\ 0 & 0 & \frac{1}{\psi_m} \end{bmatrix}, \tag{12}$$

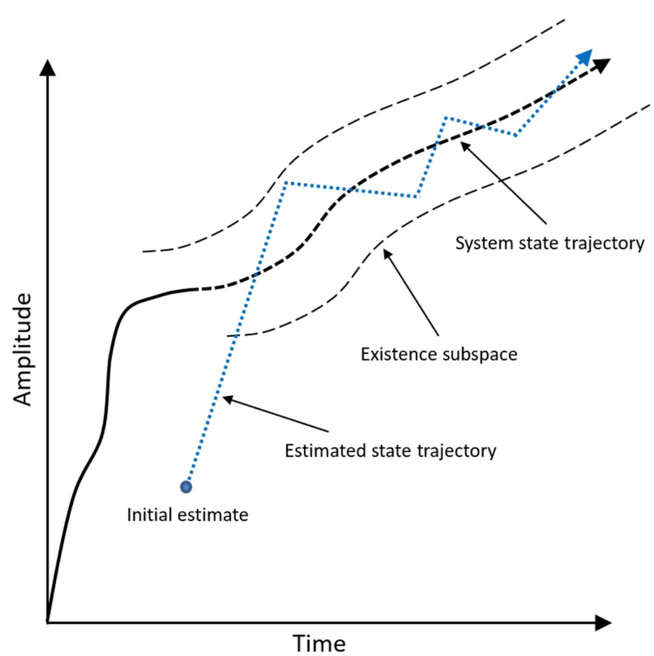

Fig. 1 The SVSF estimation concept.

where m is the number of measurements. This gain is used to calculate the updated state estimates $\hat{x}_{k+1|k+1}$ as well as the updated state error covariance matrix $P_{k+1|k+1}$, as per the KF strategy.

Finally, the updated measurement estimate $\hat{z}_{k+1|k+1}$ and measurement errors $e_{z,k+1|k+1}$ are calculated and are used in later iterations

$$\hat{z}_{k+1|k+1} = C\hat{x}_{k+1|k+1}, \tag{13}$$

$$e_{z,k+1|k+1} = z_{k+1} - \hat{z}_{k+1|k+1}. \tag{14}$$

The SVSF process results in the state estimates converging to within a region of the state trajectory.[16,8] Thereafter, it switches back and forth across the state trajectory within a region referred to as the existence subspace, as shown earlier in Fig. 1. This switching effect brings about an inherent amount of stability and robustness in the estimation process, as will be demonstrated in the simulation.

3 Square-Root Formulations

3.1 *Square-Root Kalman Filter*

The square-root formulation of the KF was developed by James Potter and Angus Andrews.[6] The method described in this section is often referred to as Potter's algorithm.[2] As per Cholesky factorization, suppose that the square root of the state error covariance matrix P is available such that $P = SS^{\mathrm{T}}$. Modifying Eq. (3) yields

$$P_{k+1|k} = S_{k+1|k}S_{k+1|k}^{\mathrm{T}} = FS_{k|k}S_{k|k}^{\mathrm{T}}F^{\mathrm{T}} + Q_k^{1/2}Q_k^{\mathrm{T}/2}. \tag{15}$$

Equation (15) is essentially Eq. (3). Modifying Eq. (4) yields

$$K_{k+1} = S_{k+1|k}S_{k+1|k}^{\mathrm{T}}H^{\mathrm{T}}(HS_{k+1|k}S_{k+1|k}^{\mathrm{T}}H^{\mathrm{T}} + R_{k+1})^{-1}. \tag{16}$$

The updated state error covariance Eq. (6) then becomes

$$P_{k+1|k+1} = (I - K_{k+1}H)S_{k+1|k}S_{k+1|k}^{\mathrm{T}}(I - K_{k+1}H)^{\mathrm{T}} + K_{k+1}R_{k+1}K_{k+1}^{\mathrm{T}}. \tag{17}$$

Alternatively, this can be written as[6]

$$P_{k+1|k+1} = S_{k+1|k}(I - a\phi\phi^{\mathrm{T}})S_{k+1|k,}^{\mathrm{T}} \tag{18}$$

where a and ϕ are defined as

$$a = (\phi^{\mathrm{T}}\phi + R_{i,k+1})^{-1}, \quad \phi = S_{k+1|k}^{\mathrm{T}}H^{\mathrm{T}}. \tag{19}$$

Note that i refers to the i'th element of the corresponding matrix or vector. As per Ref. 6, the *a posteriori* square-root covariance matrix can be calculated as follows:

$$S_{k+1|k+1} = S_{k+1|k}(I - a\gamma\phi\phi^{\mathrm{T}}), \tag{20}$$

where γ is given as[6]

$$\gamma = \left(1 + \sqrt{aR_{i,k+1}}\right). \tag{21}$$

Equations (15)–(21) can be used in conjunction with the standard KF estimation process. The main difference is that the update equation is used to update S instead of P, and the process is repeatedly iteratively.[6]

3.2 *Square-Root Smooth Variable Structure Filter*

The square-root formulation of the SVSF, hereafter referred as to SR-SVSF, is shown here.[37] It is based on the same approach as the square-root KF. For linear systems and measurements, the SR-SVSF estimation process is summarized by the following set of equations. For nonlinear systems and measurements, the nonlinearities may be linearized as per the EKF methodology. The state estimates $\hat{x}_{k+1|k}$ and square-root covariance $S_{k+1|k}$ are first calculated as follows:

$$\hat{x}_{k+1|k} = F\hat{x}_{k|k} + Gu_k, \tag{22}$$

$$S_{k+1|k}S_{k+1|k}^{\mathrm{T}} = FS_{k|k}S_{k|k}^{\mathrm{T}}F^{\mathrm{T}} + Q_k^{1/2}Q_k^{\mathrm{T}/2}. \tag{23}$$

The predicted measurement $\hat{z}_{k+1|k}$ and measurement errors $e_{z,k+1|k}$ are calculated next

$$\hat{z}_{k+1|k} = H\hat{x}_{k+1|k}, \tag{24}$$

$$e_{z,k+1|k} = z_{k+1} - \hat{z}_{k+1|k}. \tag{25}$$

Next, the gain K_{k+1} is calculated as

$$K_{k+1} = C^{+}\mathrm{diag}[(|e_{z,k+1|k}| + \gamma|e_{z,k|k}|)\mathrm{sat}(\bar{\psi}^{-1}e_{z,k+1|k})]\mathrm{diag}(e_{z,k+1|k})^{-1}. \tag{26}$$

The *a posteriori* square-root covariance matrix $S_{k+1|k+1}$ is calculated next as follows:

$$S_{k+1|k+1} = S_{k+1|k}(I - a\gamma\phi\phi^{\mathrm{T}}), \tag{27}$$

where $a = (\phi^{\mathrm{T}}\phi + R_{i,k+1})^{-1}$, $\phi = S_{k+1|k}^{\mathrm{T}}H^{\mathrm{T}}$, and $\gamma = (1 + \sqrt{aR_{i,k+1}})$. Finally, the updated measurement estimate $\hat{z}_{k+1|k+1}$ and measurement errors $e_{z,k+1|k+1}$ are calculated and are used in later iterations

$$\hat{z}_{k+1|k+1} = C\hat{x}_{k+1|k+1}, \tag{28}$$

$$e_{z,k+1|k+1} = z_{k+1} - \hat{z}_{k+1|k+1}. \tag{29}$$

The SR-SVSF estimation process is summarized by Eqs. (22)–(29). It is important to note that in this case, the gain is not affected by the square-root covariance calculation. However, the SR-SVSF formulation sets the framework for future work and implementation in other types of SVSF that rely on the covariance.[8]

4 Two-Pass Formulations

4.1 *Two-Pass Smoother*

Smoothers (whether fixed-interval, fixed-point, or fixed-lag) may be derived from the KF model. In general, as per Ref. 2, the common methodology uses the KF for measurements up to each time step that the state needs to be estimated, combined with another algorithm. The second algorithm can be derived based on running the KF backward from the last measurement to the measurement just past time t. The two independent estimates (forward and backward) can then be combined.[2]

The two-pass smoother, also known as the RTS (Rauch–Tung–Striebel) smoother, is a popular type of smoother.[1] The standard KF estimate and covariance are computed in a forward pass, and the smoothed quantities are then computed in a backward pass.[1] The forward pass is similar to the standard KF, written as follows for completeness:

$$\hat{x}_{k|k-1} = F\hat{x}_{k-1|k-1} + Gu_k, \tag{30}$$

$$P_{k|k-1} = FP_{k-1|k-1}F^{\mathrm{T}} + Q_k, \tag{31}$$

$$K_k = P_{k|k-1} H^{\mathrm{T}} (H P_{k|k-1} H^{\mathrm{T}} + R_k)^{-1}, \tag{32}$$

$$\hat{x}_{k|k} = \hat{x}_{k|k-1} + K_k (z_k - H \hat{x}_{k|k-1}), \tag{33}$$

$$P_{k|k} = (I - K_k H) P_{k|k-1} (I - K_k H)^{\mathrm{T}} + K_k R_k K_k^{\mathrm{T}}. \tag{34}$$

The backward pass is then performed using the state estimate and covariance values. The smoothed state estimate is first calculated as follows:[38]

$$\hat{x}_{k|n} = \hat{x}_{k|k} + A_k (\hat{x}_{k+1|n} - \hat{x}_{k+1|k}). \tag{35}$$

The supporting matrices are defined by[38]

$$A_k = P_{k|k-1} \bar{F}_k^{\mathrm{T}} P_{k+1|k}^{\mathrm{T}}, \tag{36}$$

$$\bar{F}_k = F - K_k H. \tag{37}$$

The smoothed state error covariance becomes[38]

$$P_{k|n} = P_{k|k} + A_k (P_{k+1|n} - P_{k+1|k}) A_k^{\mathrm{T}}. \tag{38}$$

Equations (30)–(38) summarize the two-pass smoother or the RTS algorithm. The forward pass includes the KF estimation strategy and the backward pass computes the smoothed quantities based on the available system information and measurements. The process is computed iteratively.

4.2 *Two-Pass Smooth Variable Structure Filter (Smoother)*

This paper introduces the fixed-interval formulation of the SVSF-based smoother, hereafter referred as to the variable structure smoother (VSS).[39] It is based on the same approach as the RTS or two-pass smoother. The forward pass is essentially the SVSF estimation process and is listed here for completeness

$$\hat{x}_{k|k-1} = F \hat{x}_{k-1|k-1} + G u_k, \tag{39}$$

$$P_{k|k-1} = F P_{k-1|k-1} F^{\mathrm{T}} + Q_k, \tag{40}$$

$$e_{z,k|k-1} = z_k - H \hat{x}_{k|k-1}, \tag{41}$$

$$K_k = C^{+} \mathrm{diag}[(|e_{z_{k|k-1}}| + \gamma |e_{z_{k-1|k-1}}|) \mathrm{sat}(\bar{\psi}^{-1} e_{z_{k|k-1}})] \mathrm{diag}(e_{z_{k|k-1}})^{-1}, \tag{42}$$

$$\hat{x}_{k|k} = \hat{x}_{k|k-1} + K_k (z_k - H \hat{x}_{k|k-1}), \tag{43}$$

$$P_{k|k} = (I - K_k H) P_{k|k-1} (I - K_k H)^{\mathrm{T}} + K_k R_k K_k^{\mathrm{T}}, \tag{44}$$

$$e_{z,k|k} = z_k - H \hat{x}_{k|k}. \tag{45}$$

The backward pass is then performed using the state estimate and covariance values. The smoothed state estimate is first calculated as follows:[38]

$$\hat{x}_{k|n} = \hat{x}_{k|k} + A_k (\hat{x}_{k+1|n} - \hat{x}_{k+1|k}). \tag{46}$$

The supporting matrices are defined by[38]

$$A_k = P_{k|k-1}\bar{F}_k^{\mathrm{T}} P_{k+1|k}^{\mathrm{T}}, \tag{47}$$

$$\bar{F}_k = F - K_k H. \tag{48}$$

The smoothed state error covariance becomes[38]

$$P_{k|n} = P_{k|k} + A_k (P_{k+1|n} - P_{k+1|k}) A_k^{\mathrm{T}}. \tag{49}$$

Equations (39)–(49) summarize the two-pass SVSF-based smoother or the VSS algorithm. The forward pass includes the SVSF estimation strategy with a state error covariance matrix, and the backward pass computes the smoothed quantities based on the available system information and measurements. The process is computed iteratively.

5 Target Tracking Problem for Square-Root Filters

5.1 *Target Tracking Scenario*

The target tracking problem is based on a generic air traffic control (ATC) scenario found in Ref. 4 and is as described in Ref. 8. A radar stationed at the origin provides direct position only measurements, with a standard deviation of 50 m in each coordinate. Figure 2 shows the average motion of the target.

As shown in Fig. 2, an aircraft starts from an initial position of [25,000 m, 10,000 m] at time $t = 0$ s and flies westward at 120 m/s for 125 s. The aircraft then begins a coordinated turn (CT) for a period of 90 s at a rate of deg /s. It then flies southward at 120 m/s for 125 s, followed by another CT for 30 s at 3 deg /s. The aircraft then continues to fly westward until it reaches its final destination.

In ATC scenarios, the behavior of civilian aircraft may be modeled by two different modes: uniform motion (UM), which involves a straight flight path with a constant speed and course, and maneuvering, which includes turning or climbing and descending.[4] In this case, maneuvering will refer to a CT model, where a turn is made at a constant turn rate and speed. The UM model used for this target tracking problem is given by[4,40]

$$x_{k+1} = \begin{bmatrix} 1 & 0 & T & 0 \\ 0 & 1 & 0 & T \\ 0 & 0 & 1 & 0 \\ 0 & 0 & 0 & 1 \end{bmatrix} x_k + \begin{bmatrix} \frac{1}{2}T^2 & 0 \\ 0 & \frac{1}{2}T^2 \\ T & 0 \\ 0 & T \end{bmatrix} w_k. \tag{50}$$

Note that T refers to sample rate and w_k refers to system noise. The state vector of the aircraft may be defined as

$$x_k = [\,\xi_k \quad \eta_k \quad \dot{\xi}_k \quad \dot{\eta}_k\,]^{\mathrm{T}}. \tag{51}$$

The first two states refer to the position along the x-axis and y-axis, respectively, and the last two states refer to the velocity along the x-axis and y-axis, respectively. The sampling time T used in this simulation was 5 s. When using the CT model, the state vector needs to be augmented to include the turn rate, as shown in Eq. (32).[4] The CT model may be considered nonlinear if the turn rate of the aircraft is not known. Note that a left turn corresponds to a positive turn rate and a right turn has a negative turn rate. This sign convention follows the commonly used trigonometric convention (the opposite is true for navigation convention).[4] As per Refs. 4 and 40, the CT model is given by Eq. (53)

$$x_k = [\,\xi_k \quad \eta_k \quad \dot{\xi}_k \quad \dot{\eta}_k \quad \omega_k\,]^{\mathrm{T}}, \tag{52}$$

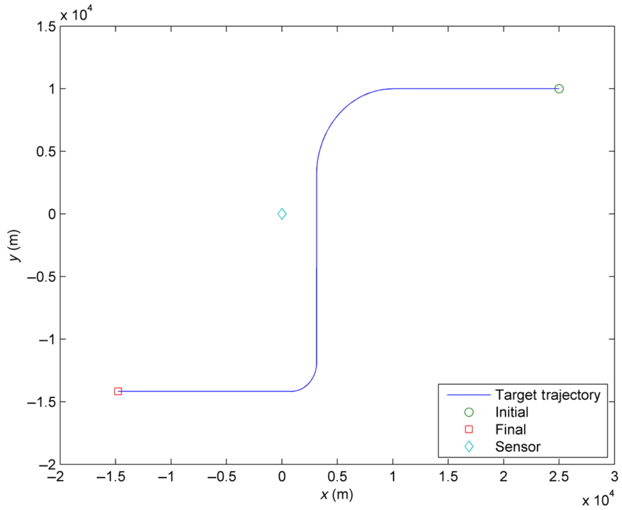

Fig. 2 True target trajectory for the nonlinear estimation target tracking problem.

$$x_{k+1} = \begin{bmatrix} 1 & 0 & \frac{\sin \omega_k T}{\omega_k} & -\frac{1-\cos \omega_k T}{\omega_k} & 0 \\ 0 & 1 & \frac{1-\cos \omega_k T}{\omega_k} & \frac{\sin \omega_k T}{\omega_k} & 0 \\ 0 & 0 & \cos \omega_k T & -\sin \omega_k T & 0 \\ 0 & 0 & \sin \omega_k T & \cos \omega_k T & 0 \\ 0 & 0 & 0 & 0 & 1 \end{bmatrix} x_k + \begin{bmatrix} \frac{1}{2}T^2 & 0 & 0 \\ 0 & \frac{1}{2}T^2 & 0 \\ T & 0 & 0 \\ 0 & T & 0 \\ 0 & 0 & T \end{bmatrix} w_k. \tag{53}$$

Since the radar stationed at the origin provides direct position measurements only, the measurement equation may be formed linearly as follows:

$$z_k = \begin{bmatrix} 1 & 0 & 0 & 0 & 0 \\ 0 & 1 & 0 & 0 & 0 \end{bmatrix} x_k + v_k. \tag{54}$$

Note that v_k refers to measurement noise. Equations (50)–(54) were used to generate the true state values of the trajectory and the radar measurements for this target tracking scenario. As previously mentioned, the EKF uses a linearized form of the system and measurement matrices. In this case, the system defined by Eq. (53) is nonlinear such that the Jacobian of it yields a linearized form as shown in Eq. (55). The terms in the last column of Eq. (55) are correspondingly defined in Eq. (56)[4]

$$\left[\nabla_x F_{k,x}^T \right]^T \Big|_{x_k=\hat{x}_k} = \begin{bmatrix} 1 & 0 & \frac{\sin \hat{\omega}_k T}{\hat{\omega}_k} & -\frac{1-\cos \hat{\omega}_k T}{\hat{\omega}_k} & F_{\hat{\omega}1} \\ 0 & 1 & \frac{1-\cos \hat{\omega}_k T}{\hat{\omega}_k} & \frac{\sin \hat{\omega}_k T}{\hat{\omega}_k} & F_{\hat{\omega}2} \\ 0 & 0 & \cos \hat{\omega}_k T & -\sin \hat{\omega}_k T & F_{\hat{\omega}3} \\ 0 & 0 & \sin \hat{\omega}_k T & \cos \hat{\omega}_k T & F_{\hat{\omega}4} \\ 0 & 0 & 0 & 0 & 1 \end{bmatrix}, \tag{55}$$

$$\begin{bmatrix} F_{\hat{\omega}1} \\ F_{\hat{\omega}2} \\ F_{\hat{\omega}3} \\ F_{\hat{\omega}4} \end{bmatrix} = \begin{bmatrix} \frac{(\cos \hat{\omega}_k T)T}{\hat{\omega}_k} \widehat{\dot{\xi}_k} - \frac{(\sin \hat{\omega}_k T)}{\hat{\omega}_k^2} \widehat{\dot{\xi}_k} - \frac{(\sin \hat{\omega}_k T)T}{\hat{\omega}_k} \widehat{\dot{\eta}_k} - \frac{(-1+\cos \hat{\omega}_k T)}{\hat{\omega}_k^2} \widehat{\dot{\eta}_k} \\ \frac{(\sin \hat{\omega}_k T)T}{\hat{\omega}_k} \widehat{\dot{\xi}_k} - \frac{(1-\cos \hat{\omega}_k T)}{\hat{\omega}_k^2} \widehat{\dot{\xi}_k} - \frac{(\cos \hat{\omega}_k T)T}{\hat{\omega}_k} \widehat{\dot{\eta}_k} - \frac{(\sin \hat{\omega}_k T)}{\hat{\omega}_k^2} \widehat{\dot{\eta}_k} \\ -(\sin \hat{\omega}_k T)T \widehat{\dot{\xi}_k} - (\cos \hat{\omega}_k T)T \widehat{\dot{\eta}_k} \\ (\cos \hat{\omega}_k T)T \widehat{\dot{\xi}_k} - (\sin \hat{\omega}_k T)T \widehat{\dot{\eta}_k} \end{bmatrix}. \tag{56}$$

To generate the results for this section, the following values were used for the initial state error covariance matrix $P_{0|0}$, the system noise matrix Q, and the measurement noise matrix R

$$P_{0|0} = \begin{bmatrix} R_{11} & 0 & 0 & 0 & 0 \\ 0 & R_{22} & 0 & 0 & 0 \\ 0 & 0 & 100 & 0 & 0 \\ 0 & 0 & 0 & 100 & 0 \\ 0 & 0 & 0 & 0 & 1 \end{bmatrix}, \tag{57}$$

$$Q = L_1 \begin{bmatrix} \frac{T^3}{3} & 0 & \frac{T^2}{2} & 0 & 0 \\ 0 & \frac{T^3}{3} & 0 & \frac{T^2}{2} & 0 \\ \frac{T^2}{2} & 0 & T & 0 & 0 \\ 0 & \frac{T^2}{2} & 0 & T & 0 \\ 0 & 0 & 0 & 0 & \frac{L_2}{L_1} T \end{bmatrix}, \tag{58}$$

$$R = 50^2 \begin{bmatrix} 1 & 0 \\ 0 & 1 \end{bmatrix}. \tag{59}$$

Note that L_1 and L_2 are referred to as power spectral densities and were defined as 0.16 and 0.01, respectively.[40] The system and measurement noise (w_k and v_k) were generated using their respective covariance values (Q and R). Also, when using the UM model, the fifth row and column of Eqs. (57) and (58) were truncated. For the stand-alone SVSF estimation process, the limit on the smoothing boundary layer widths were defined as $\psi = [500 \quad 1000 \quad 500 \quad 1000 \quad 1]^T$, and the SVSF "memory" or convergence rate was set to $\gamma = 0.1$. These parameters were tuned based on some knowledge of the uncertainties (i.e., magnitude of noise) and with the goal of decreasing the estimation error. It is required to transform the measurement matrix into a square matrix (i.e., identity) such that an "artificial" measurement is created. It is possible to derive "artificial" velocity measurements based on the available position measurements. For example, consider the following artificial measurement vector y_k for the SVSF:

$$y_k = \begin{bmatrix} z_{1,k} \\ z_{2,k} \\ (z_{1,k+1} - z_{1,k})/T \\ (z_{2,k+1} - z_{2,k})/T \\ 0 \end{bmatrix}. \tag{60}$$

The accuracy of Eq. (60) depends on the sampling rate T. Applying the above type of transformation to nonmeasured states allows a measurement matrix equivalent to the identity matrix. The estimation process would continue as in the previous section, where $H = I$. Note, however, that the artificial velocity measurements would be delayed one time step. Furthermore, it is assumed that the artificial turn rate measurement is set to 0 since no artificial measurement could be created based on the available measurements. A total of 500 Monte Carlo runs were performed, and the results were averaged.

5.2 *Results*

Both the square-root KF and the proposed SR-SVSF were applied on the target tracking problem. The algorithms were applied to the aforementioned setup. The target tracking results are shown in Fig. 3. The square-root-based SVSF was able to follow the target trajectory, regardless of which flight model was implemented. However, the square-root-based EKF experienced difficulty at the presence of the aircraft turns. This is primarily due to the difference between the model used by the filter and the model actually experienced by the target. The estimation error is shown in Fig. 4. Notice how the SR-SVSF yielded relatively similar results, regardless of which model was implemented. This is primarily due to the robust estimation process inherent to the switching gain. A second case was studied in which the measurement at 50 s was increased by 1000 times. This case further demonstrated the robustness of the SR-SVSF. The SR-EKF was unable to overcome the measurement error; however, the SR-SVSF was able to maintain the true state trajectory. This is further shown in Figs. 5 and 6.

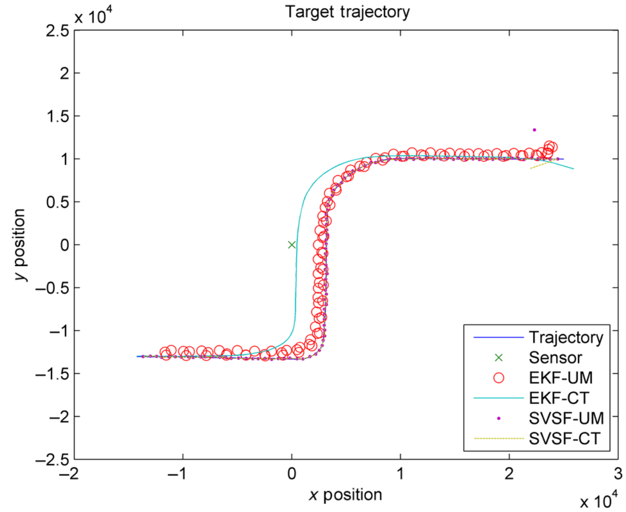

Fig. 3 True and estimated target trajectories for the nonlinear estimation problem.

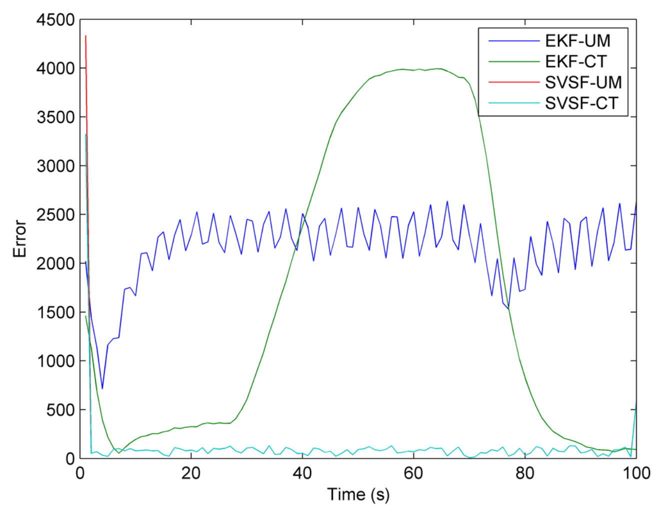

Fig. 4 Estimation errors for the nonlinear estimation problem.

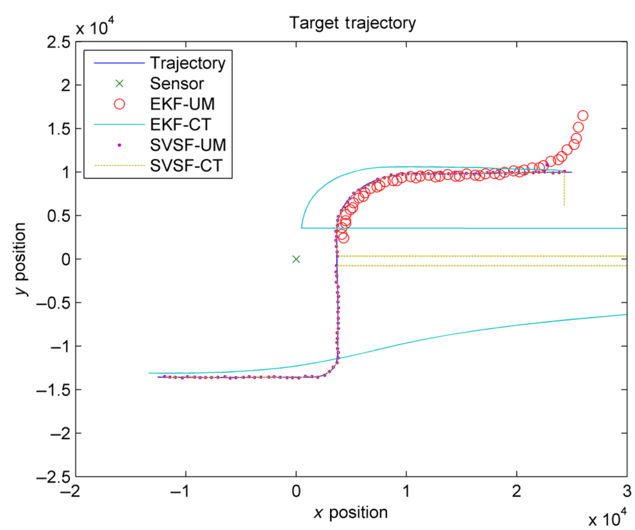

Fig. 5 True and estimated target trajectories with the presence of measurement errors.

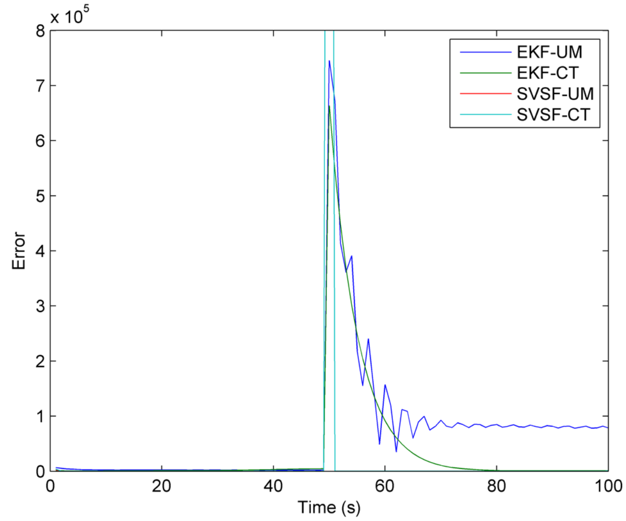

Fig. 6 Estimation errors for the square-root filters with the presence of measurement errors.

6 Electrohydrostatic Actuator Estimation Problem for Two-Pass Smoothers

6.1 *Aerospace Actuator Scenario*

In this section, an electrohydrostatic actuator (EHA) is described. It is important to note that smoothers are typically used in applications that can have offline calculations or some estimation delay. However, this example uses computer simulations to allow a detailed investigation of the effects of the smoothers and parametric uncertainties. The EHA model is based on an actual prototype built for experimentation and is commonly used as an aerospace flight surface actuator.[16,15] The EHA has been modeled as a third-order linear system with state variables related to its position, velocity, and acceleration.[16] Initially, it is assumed that all three states have measurements associated with them (i.e., $C = I$). The sample time of the system is $T = 0.001$ s, and the discrete-time state space system equation may be defined as follows:[16]

$$x_{k+1} = \begin{bmatrix} 1 & 0.001 & 0 \\ 0 & 1 & 0.001 \\ -557.02 & -28.616 & 0.9418 \end{bmatrix} x_k + \begin{bmatrix} 0 \\ 0 \\ 557.02 \end{bmatrix} u_k. \tag{61}$$

For this case, the corresponding measurement equation is defined by

$$z_{k+1} = \begin{bmatrix} 1 & 0 & 0 \\ 0 & 1 & 0 \\ 0 & 0 & 1 \end{bmatrix} x_{k+1}. \tag{62}$$

The initial state values are set to zero. The system and measurement noises (w and v) are considered to be Gaussian, with zero mean and variances Q and R, respectively. The initial state error covariance $P_{0|0}$, system noise covariance Q, and measurement noise covariance R are defined, respectively, as follows:

$$P_{0|0} = 10Q, \tag{63}$$

$$Q = \begin{bmatrix} 1\times 10^{-5} & 0 & 0 \\ 0 & 1\times 10^{-3} & 0 \\ 0 & 0 & 1\times 10^{-1} \end{bmatrix}, \tag{64}$$

$$R = \begin{bmatrix} 1 \times 10^{-4} & 0 & 0 \\ 0 & 1 \times 10^{-2} & 0 \\ 0 & 0 & 1 \end{bmatrix}. \tag{65}$$

As per Ref. 41, for the standard SVSF estimation process, the "memory" or convergence rate was set to $\gamma = 0.1$, and the limits for the smoothing boundary layer widths (diagonal elements) were defined as $\psi = [0.05 \quad 0.5 \quad 5]^{\mathrm{T}}$. These parameters were selected based on the distribution of the system and measurement noises. For example, the limit for the smoothing boundary layer width ψ was set to 5 times the maximum system noise, or approximately equal to the measurement noise. The initial state estimates for the filters were defined randomly by a normal distribution, around the true initial state values x_0 and using the initial state error covariance $P_{0|0}$. Two different cases were studied in this section. The first case was considered "normal," and the second included a system modeling error halfway through the simulation. A total of 500 Monte Carlo runs were performed, and the results were averaged.

6.2 *Results*

Figures 7–9 show the result of applying the Kalman-based smoother (labeled as KS) and the variable structure smoother (labeled as VSS). Both the KS and VSS were able to smooth out the kinematic states. However, the KS performed slightly better in terms of accuracy, as expected. The position root mean square error (RMSE) for the KS and VSS was 0.0019 and 0.0023 m, respectively. The velocity RMSE for the KS and VSS was 0.0216 and 0.0269 m/s, respectively. Finally, the acceleration RMSE was closer and was found for the KS and VSS as 0.3199 and 0.3202 $\mathrm{m/s^2}$, respectively.

As per Ref. 16, consider the introduction of modeling error or uncertainty such that the system used by the smoothers is modified Eq. (66) at 0.5 s. The model changes at this point to coincide with the input step, exaggerating the effects of modeling uncertainty. Figures 10–12 show the result of applying the KS and VSS on the system with modeling uncertainty halfway through the simulation. The KS failed to yield a good position estimate but was able to follow (somewhat) the velocity and acceleration trajectories. The VSS was able to overcome the uncertainties and yielded accurate and robust state estimates

$$x_{k+1} = \begin{bmatrix} 1 & 0.001 & 0 \\ 0 & 1 & 0.001 \\ -240 & -28 & 0.9418 \end{bmatrix} x_k + \begin{bmatrix} 0 \\ 0 \\ 557.02 \end{bmatrix} u_{k.} \tag{66}$$

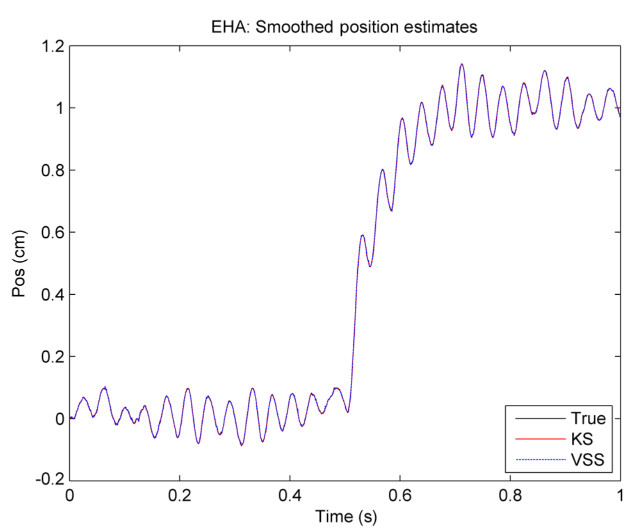

Fig. 7 Smoothed position estimates of the EHA by the KS and VSS.

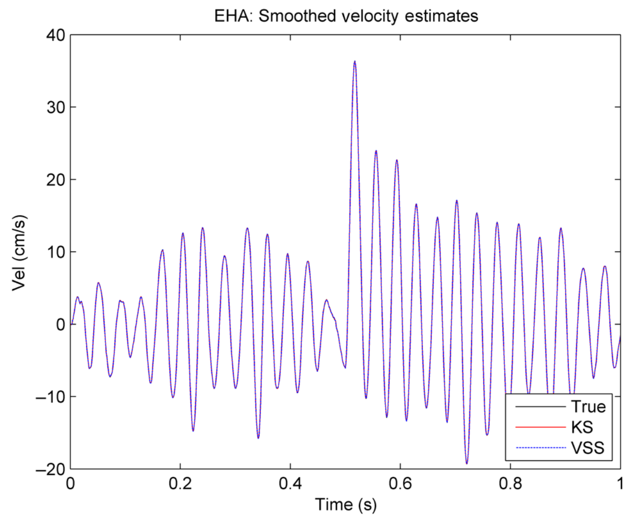

Fig. 8 Smoothed velocity estimates of the EHA by the KS and VSS.

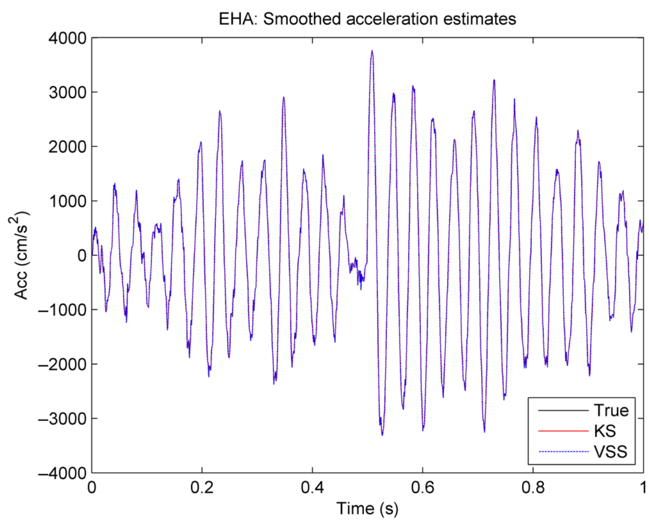

Fig. 9 Smoothed acceleration estimates of the EHA by the KS and VSS.

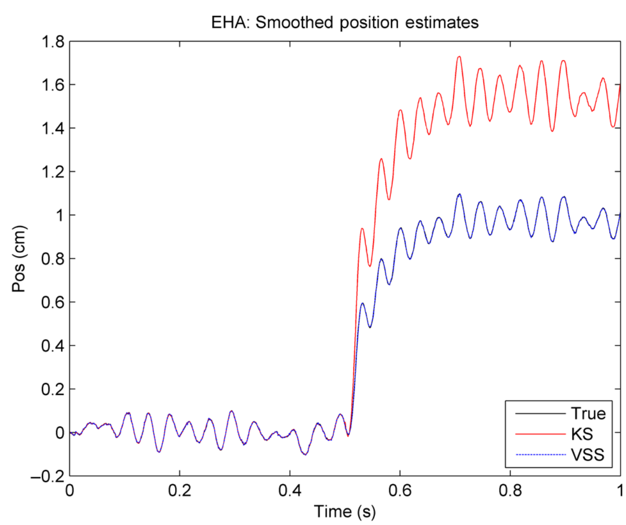

Fig. 10 Smoothed position estimates of the EHA by the KS and VSS (with uncertainties).

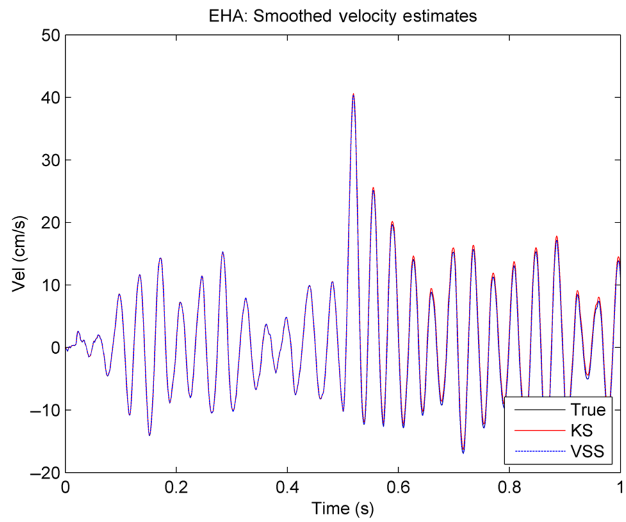

Fig. 11 Smoothed velocity estimates of the EHA by the KS and VSS (with uncertainties).

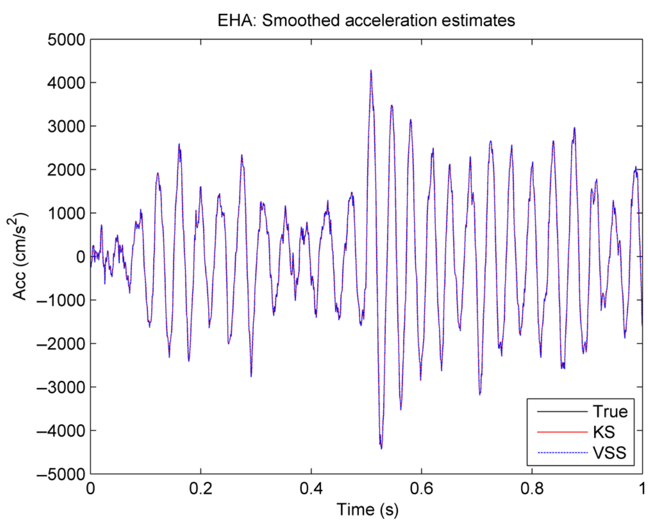

Fig. 12 Smoothed acceleration estimates of the EHA by the KS and VSS (with uncertainties).

7 Conclusions

This paper introduced a two-pass, SVSF-based smoother for the purpose of state and parameter estimation. The proposed algorithm was applied to a linear flight surface actuator and was compared with the popular KF-based smoother. For the computer experiment, under normal conditions, both the two-pass smoother and the proposed VSS performed well. During the presence of modeling uncertainties, the VSS was able to overcome inaccuracies and yield a stable solution. In addition, this paper introduced a new version of the SVSF based on Potter's square-root algorithm. The new methodology, referred to simply as the SR-SVSF, was applied on a nonlinear target tracking problem. The results were compared with the popular Kalman filter strategy. It was determined that the robustness of the SVSF switching gain yielded a stable and accurate estimation of the target. The estimates were found to be bounded to the true state trajectory. With the presence of measurement errors, the KF-based strategy failed to yield a good result; however, the SVSF-based strategy remained stable. Future studies will look at implementing the VSS and SR-SVSF on real-life data and benchmark problems.

Appendix: Proof of SVSF Stability

The SVSF guarantees stability by making use of a Lyapunov stability condition.[16] According to Lyapunov stability theory, a Lyapunov function V is said to be stable if V is locally positive definite and the time derivative of V is locally negative semidefinite. Let V be a Lyapunov function defined in terms of the SVSF *a posteriori* estimation error such that

$$V = e^{\mathrm{T}}_{z,k+1|k+1} e_{z,k+1|k+1} > 0. \tag{67}$$

According to Lyapunov stability theory, the estimation process is stable if the following is satisfied:[42]

$$\Delta V \leq 0, \tag{68}$$

where ΔV represents the change in the Lyapunov function, and, in this case, is defined as

$$\Delta V = e^{\mathrm{T}}_{z,k+1|k+1} e_{z,k+1|k+1} - e^{\mathrm{T}}_{z,k|k} e_{z,k|k}. \tag{69}$$

Substituting Eq. (69) into (68) and rearranging yields

$$e^{\mathrm{T}}_{z,k+1|k+1} e_{z,k+1|k+1} < e^{\mathrm{T}}_{z,k|k} e_{z,k|k}. \tag{70}$$

Equation (70) is equivalent to the following, which is the stability condition for the SVSF:[16]

$$|e_{z,k+1|k+1}|_{\mathrm{Abs}} < |e_{z,k|k}|_{\mathrm{Abs}}. \tag{71}$$

To remove the absolute operator in Eq. (71), both sides are expressed in the form of diagonal matrices [i.e., $\mathrm{diag}(e)$], as follows:

$$\mathrm{diag}(e_{z,k+1|k+1})\mathrm{diag}(e_{z,k+1|k+1}) < \mathrm{diag}(e_{z,k|k})\mathrm{diag}(e_{z,k|k}). \tag{72}$$

Assuming that the measurement function is well-defined (and it may be linearized as C), then the *a posteriori* measurement error may be calculated as

$$e_{z,k+1|k+1} = Ce_{x,k+1|k+1} + v_{k+1}. \tag{73}$$

Substitution of Eq. (73) into (72) yields

$$\begin{pmatrix} \mathrm{diag}(Ce_{x,k+1|k+1})\mathrm{diag}(Ce_{x,k+1|k+1}) \\ +\mathrm{diag}(v_{k+1})\mathrm{diag}(v_{k+1}) \\ +\mathrm{diag}(Ce_{x,k+1|k+1})\mathrm{diag}(v_{k+1}) \\ +\mathrm{diag}(v_{k+1})\mathrm{diag}(Ce_{x,k+1|k+1}) \end{pmatrix} < \begin{pmatrix} \mathrm{diag}(Ce_{x,k|k})\mathrm{diag}(Ce_{x,k|k}) \\ +\mathrm{diag}(v_k)\mathrm{diag}(v_k) \\ +\mathrm{diag}(Ce_{x,k|k})\mathrm{diag}(v_k) \\ +\mathrm{diag}(v_k)\mathrm{diag}(Ce_{x,k|k}) \end{pmatrix}. \tag{74}$$

If the measurement noise v_{k+1} is stationary white, then taking the expectation of both sides in Eq. (74) and simplifying yields the following:

$$E\begin{bmatrix} \mathrm{diag}(Ce_{x,k+1|k+1})\mathrm{diag}(Ce_{x,k+1|k+1}) \\ +\mathrm{diag}(v_{k+1})\mathrm{diag}(v_{k+1}) \end{bmatrix} < E\begin{bmatrix} \mathrm{diag}(Ce_{x,k|k})\mathrm{diag}(Ce_{x,k|k}) \\ +\mathrm{diag}(v_k)\mathrm{diag}(v_k) \end{bmatrix}, \tag{75}$$

where $E[\mathrm{diag}(Ce_{x,k+1|k+1})\mathrm{diag}(v_{k+1})]$ and $E[\mathrm{diag}(v_k)\mathrm{diag}(Ce_{x,k|k})]$ vanish due to the white noise assumption. For a diagonal, positive, and time-invariant measurement matrix, Eq. (75) becomes

$$E[\mathrm{diag}(e_{x,k+1|k+1})\mathrm{diag}(e_{x,k+1|k+1})] < E[\mathrm{diag}(e_{x,k|k})\mathrm{diag}(e_{x,k|k})]. \tag{76}$$

Note that the assumptions pertaining to the measurement matrix are realistic since most applications use linear sensors as feedback in their operations. Moreover, these sensors are well calibrated, and their structures are well-known.[16] Finally, Eq. (76) becomes

$$E(|e_{x,k+1|k+1}|_{\mathrm{Abs}}) < E(|e_{x,k|k}|_{\mathrm{Abs}}). \tag{77}$$

Equation (77) is the proof of stability for the SVSF. It states that the expectation of the *a posteriori* estimation error is reduced over time (i.e., converges toward a region of the state trajectory referred to as the existence subspace). Furthermore, the proof of stability may be used to derive the SVSF gain K_{k+1}. Define γ to be a diagonal matrix with elements $0 < \gamma_{ii} \leq 1$ such that

$$|e_{z,k|k}|_{\mathrm{Abs}} > \gamma|e_{z,k|k}|_{\mathrm{Abs}}. \tag{78}$$

Adding the absolute value of the *a priori* measurement error $|e_{z,k+1|k}|_{\mathrm{Abs}}$ to both sides of Eq. (78) yields

$$|e_{z,k+1|k}|_{\mathrm{Abs}} + |e_{z,k|k}|_{\mathrm{Abs}} > |e_{z,k+1|k}|_{\mathrm{Abs}} + \gamma|e_{z,k|k}|_{\mathrm{Abs}}. \tag{79}$$

The absolute value of the measurement matrix multiplied with the SVSF gain $|CK_{k+1}|_{\mathrm{Abs}}$ is set equal to the right side of Eq. (79) such that[42]

$$|CK_{k+1}|_{\mathrm{Abs}} = |e_{z,k+1|k}|_{\mathrm{Abs}} + \gamma|e_{z,k|k}|_{\mathrm{Abs}}. \tag{80}$$

Next, consider the following definition:

$$|CK_{k+1}|_{\mathrm{Abs}} = CK_{k+1}\mathrm{sign}(CK_{k+1}). \tag{81}$$

Furthermore, the sign of the measurement matrix multiplied with the SVSF gain CK_{k+1} is set equal to the sign of the *a priori* measurement error $e_{z,k+1|k}$.[16,42] This leads to the SVSF gain (with a sign function), as follows:

$$K_{k+1} = C^{+}(|e_{z,k+1|k}|_{\mathrm{Abs}} + \gamma|e_{z,k|k}|_{\mathrm{Abs}})\mathrm{sign}(e_{z,k+1|k}). \tag{82}$$

Note that Eq. (82) satisfies and is derived from inequality Eq. (80), and for $0 < \gamma_{ii} \leq 1$, it satisfies Eq. (80) with the stability condition Eq. (71), as per Refs. 16 and 42.

References

1. B. D. O. Anderson and J. B. Moore, *Optimal Filtering*, Prentice-Hall, Englewood Cliffs, New Jersey (1979).
2. M. S. Grewal and A. P. Andrews, *Kalman Filtering: Theory and Practice Using MATLAB*, 3rd ed., John Wiley and Sons, Inc., New York (2008).
3. A. Gelb, *Applied Optimal Estimation*, MIT Press, Cambridge, Massachusetts (1974).
4. Y. Bar-Shalom, X. Rong Li, and T. Kirubarajan, *Estimation with Applications to Tracking and Navigation*, John Wiley and Sons, Inc., New York (2001).
5. M. S. Grewal and K. James, "Kalman filter implementation with improved numerical properties," *IEEE Trans. Autom. Control* **55**(9), 2058–2068 (2010).
6. D. Simon, *Optimal State Estimation: Kalman, H-Infinity, and Nonlinear Approaches*, Wiley-Interscience, New York (2006).
7. R. E. Kalman, "A new approach to linear filtering and prediction problems," *J. Basic Eng. Trans. ASME* **82**, 35–45 (1960).
8. S. A. Gadsden, "Smooth variable structure filtering: theory and applications," PhD Thesis, McMaster University, Hamilton, Ontario (2011).
9. S. A. Gadsden and S. R. Habibi, "A new form of the smooth variable structure filter with a covariance derivation," in *IEEE Conf. on Decision and Control*, Atlanta, Georgia (2010).
10. S. J. Julier, J. K. Ulhmann, and H. F. Durrant-Whyte, "A new method for nonlinear transformation of means and covariances in filters and estimators," *IEEE Trans. Autom. Control* **45**, 477–482 (2000).
11. S. A. Gadsden, S. R. Habibi, and T. Kirubarajan, "Kalman and smooth variable structure filters for robust estimation," *IEEE Trans. Aerosp. Electron. Syst.* **50**(2), 1038–1050 (2014).

12. S. A. Gadsden et al., "Combined cubature Kalman and smooth variable structure filtering: a robust estimation strategy," *Signal Process.* **96**(B), 290–299 (2014).
13. B. Hassibi and T. Kailath, "H-infinity adaptive filtering," in *IEEE Int. Conf. on Acoustics, Speech, and Signal Processing* (1995).
14. S. R. Habibi and R. Burton, "The variable structure filter," *ASME J. Dyn. Syst. Meas. Control* **125**, 287–293 (2003).
15. S. R. Habibi and R. Burton, "Parameter identification for a high performance hydrostatic actuation system using the variable structure filter concept," *ASME J. Dyn. Syst. Meas. Control* **129**(2), 229–235 (2007).
16. S. R. Habibi, "The smooth variable structure filter," *Proc. IEEE* **95**(5), 1026–1059 (2007).
17. M. Al-Shabi, "The general toeplitz/observability SVSF," PhD Thesis, McMaster University, Hamilton, Ontario (2011).
18. S. A. Gadsden, Y. Song, and S. R. Habibi, "Novel model-based estimators for the purposes of fault detection and diagnosis," *IEEE/ASME Trans. Mechatron.* **18**(4), 1237–1249 (2013).
19. V. I. Utkin, *Sliding Mode and Their Application in Variable Structure Systems*, English Translation ed., Mir Publication (1978).
20. S. A. Gadsden et al., "Nonlinear estimation techniques applied on target tracking problems," *ASME J. Dyn. Syst. Meas. Control* **134**(5), 054501 (2012).
21. S. A. Gadsden et al., "Friction fault detection of an electrohydrostatic actuator," in *ASME/Bath Symp. on Fluid Power and Motion Control (FPMC)*, Washington, D.C. (2011).
22. V. Jouppila et al., "Sliding mode controller and filter applied to a pneumatic mckibben muscle actuator," in *ASME Int. Mechanical Engineering Congress and Exposition (IMECE)*, Lake Buena Vista, Florida (2009).
23. J. E. Potter and R. G. Stern, "Statistical filtering of space navigation measurements," in *Proc. of 1963 AIAA Guidance and Control Conf.*, New York (1963).
24. N. A. Carlson, "Fast triangular formulation of the square root filter," *AIAA J.* **11**(9), 1259–1265 (1973).
25. G. J. Bierman, *Factorization Methods for Discrete Sequential Estimation*, Academic Press, Inc., New York (1977).
26. R. Van der Merwe and E. A. Wan, "The square-root unscented kalman filter for state and parameter-estimation," in *IEEE Int. Conf. on Acoustics, Speech, and Signal Processing* (2001).
27. W. H. Press et al., *Numerical Recipes: The Art of Scientific Computing*, Cambridge University Press, New York (2007).
28. K. Lemon and B. W. Welch, *Comparison of Nonlinear Filtering Techniques for Lunar Surface Roving Navigation*, NASA, Cleveland, Ohio (2008).
29. G. J. Bierman, "Measurement updating using the U-D factorization," in *IEEE Conf. on Decision and Control* (1975).
30. C. L. Thornton and G. J. Bierman, "Givens transformation techniques for Kalman filtering," *Acta Astronaut.* **4**(7–8), 847–863 (1977).
31. A. Andrews, "A square root formulation of the Kalman covariance equations," *AIAA J.* **6**, 1165–1166 (1968).
32. J. M. Bennet, "Triangular factors of modified matrices," *Numerische Mathematik* **7**, 217–221 (1963).
33. S. Haykin, *Kalman Filtering and Neural Networks*, John Wiley and Sons, Inc., New York (2001).
34. S. A. Gadsden et al., "Application of the smooth variable structure filter to a multi-target tracking problem," in *Signal Processing, Sensor Fusion, and Target Recognition, Society of Photo-Optical Instrumentation Engineers (SPIE)*, Orlando, Florida (2011).
35. S. A. Gadsden, S. R. Habibi, and T. Kirubarajan, "A novel interacting multiple model method for target tracking," in *13th Int. Conf. on Information Fusion*, Edinburgh, UK (2010).
36. G. Welch and G. Bishop, "An introduction to the Kalman filter," TR 95-041, Department of Computer Science, University of North Carolina, Chapel Hill, North Carolina, http://www.cs.unc.edu/~welch/media/pdf/kalman_intro.pdf (24 July 2006).

37. S. A. Gadsden, M. Al-Shabi, and T. Kirubarajan, "Square-root formulation of the SVSF with applications to nonlinear target tracking problems," *Proc. SPIE* **9474**, 947408 (2015).
38. N. Shimkin, *Optimal Smoothing: Estimation and Identification in Dynamical Systems*, Israel Institute of Technology, Department of Electrical Engineering, Haifa, Israel (2009).
39. S. A. Gadsden, M. Al-Shabi, and T. Kirubarajan, "Two-pass smoother based on the SVSF estimation strategy," *Proc. SPIE* **9474**, 947409 (2015).
40. H. Wang, T. Kirubarajan, and Y. Bar-Shalom, "Precision large scale air traffic surveillance using an IMM estimator with assignment," *Trans. IEEE Aerosp. Electron. Syst. J.* **35**(1), 255–266 (1999).
41. S. A. Gadsden and S. R. Habibi, "A new robust filtering strategy for linear systems," *ASME J. Dyn. Syst. Meas. Control* **135**(1) (2012).
42. M. Al-Shabi, *The General Toeplitz/Observability SVSF*, PhD Thesis, McMaster University, Hamilton, Ontario (2011).

S. Andrew Gadsden completed his PhD in mechanical engineering at McMaster University in 2011. He is an assistant professor in the School of Engineering, University of Guelph, Ontario, Canada, and is director of the Intelligent Control and Estimation (ICE) Research Laboratory. His research and teaching interests include mechatronics and robotics, control and estimation theory, and intelligent or cognitive systems. He is an ASME and IEEE member, project management professional, and a professional engineer of Ontario.

Andrew S. Lee is currently a graduate student in the Department of Mechanical Engineering, University of Maryland, Baltimore, Maryland, USA. His expected MS graduation date is summer 2017. In addition to his scholarly activities, he lectures a fourth-year control systems course in the mechanical engineering undergraduate curriculum. He plans to attend the University of Guelph to pursue his PhD in the area of intelligent estimation theory.